Chapter 2
Review of Telecommunication Aspects for Power Amplifier Design

In this chapter RF and microwave telecommunication theory, together with semiconductor and substrate theory, as applicable to power amplifier design, is presented to complement the basic theory of power amplifiers presented in Chap. 1. Several topics are addressed.

The chapter starts with a review of the frequency spectrum and various transmission bands and their implications for transceiver system design. The feasibility of passive component implementations in each frequency range is investigated and power amplifiers are placed into the context of the transceiver system. A review of various digital modulation schemes, commonly used with power amplifiers, is also presented.

Secondly, the theory behind transistor operation under large-signal and high power is discussed. Different transistor types are discussed and their advantages and disadvantages compared to other types are listed. In addition, various semiconductor fabrication technologies are compared for complete system integration or just for active device (transistor) integration. This is complemented by a discussion of different substrates for discrete implementations, PCBs and packaging. Heating presents a typical problem when large amounts of power are dissipated, thus temperature aspects of transistors and semiconductor materials are also discussed.

Last part of this chapter focuses on the scattering (*S*-) parameters and admittance (*Y*-) parameters review, Smith charts and some other aspects of RF and microwave engineering, such as resonance, loaded quality factor, bandwidth, insertion loss and impedance transformation. Fourier analysis of periodic signals is also discussed.

2.1 Wavelength and Transmission Bands

Frequency of operation has a major influence on the behavior of passive and active devices. Below 30 GHz, transceivers constructed by lumped elements can be more compact than designs based on transmission lines. Above 30 GHz, transceivers and their elements require accurate modeling and high-precision manufacturing. Above 60 GHz, transmission lines and waveguides are more practical. As described in Chap. 1, this book presents a design methodology for power amplifiers up to

M. Božanić and S. Sinha, *Power Amplifiers for the S-, C-, X- and Ku-bands*,
Signals and Communication Technology, DOI 10.1007/978-3-319-28376-0_2

Ku-band, the top end of which is located at 18 GHz [1–3]. Thus, the classification of the different bands in the frequency spectrum is beneficial for power amplifier design and is included in this section. Frequency bands are defined by the international telecommunication union [4].

The frequency is related to wavelength according to relation

$$\lambda = \frac{v}{f}, \tag{2.1}$$

where v is the phase speed of the wave and f is the wave frequency. The phase speed of the electromagnetic wave is the speed of light, which is about 3×10^8 m/s. At lower frequencies, the wavelengths of signals are very large, so the size of the electrical components has little impact on these signals. At 2.4 GHz, the wavelength is 12.5 cm. This means that any component or a connection should not be greater than a tenth of the wavelength (12.5 mm) for a system to behave with minimal loss. This can still be accomplished on a PCB. At 18 GHz, the wavelength is 1.7 cm and transmission lines can only be avoided on chip without incurring mismatches due to connections longer than about 1/10 of the wavelength. In all other cases, careful matching is paramount.

The extremely low frequency (ELF), voice frequency (VF) and very-low-frequency (VLF) ranges span from 30 to 30 kHz and contain audible frequencies and are thus not suitable for radio transmission. Low frequencies (LF) span from 30 to 300 kHz and are used for long-range navigation, submarine communication and telegraphy. Medium frequencies (MF) or medium waves span from 300 to 3 MHz and are used for commercial radio. The high-frequency (HF) range with frequencies from 3 to 30 MHz is used for military tactical radios and for amateur radio operators because of the long-distance propagation properties of the waves with 30-m-long waves.

The very-high-frequency (VHF) range with frequencies from 30 to 300 MHz and the UHF range with frequencies from 300 to 3 GHz are used for television broadcast, cordless and cellular telephone transmission, as well as for other wireless applications, such as wireless local area networks (WLANs) and Bluetooth®. This is also suitable for industrial heating and microwave ovens.

The SHF range includes frequencies from 3 to 30 GHz and the extremely-high-frequency (EHF) range includes frequencies from 30 to 300 GHz. These two ranges are mostly used for satellite communication and radar applications.

UHF, SHF and EHF frequency ranges are further divided into *L*-band (1–2 GHz), *S*-band (2–4 GHz), *C*-band (4–8 GHz), *X*-band (8–12.4 GHz), *K*-band (18–26.5 GHz), *Ku*-band (26.5–40 GHz), *V*-band (40–75 GHz) and *W*-band (75–110 GHz). Informally, the spectrum is also divided into RF, microwave and mm-waves, with the boundaries between the three bands somewhat loosely defined. The frequency spectrum is illustrated in Table 2.1. This table also shows the feasibility of passives as applicable to each frequency range.

Table 2.1 The frequency spectrum and feasibility of passives

Frequency range	Wavelength range	Range name	UHF/SHF/EHF band name	Other names/feasibility of passives
30–300 Hz	10,000–1000 km	ELF	–	No transmission
300–3000 Hz	1000–100 km	VF		
3–30 kHz	100–10 km	VLF		RF/lumped passives
30–300 kHz	10–1 km	LF		
300–3000 kHz	1000–100 m	MF		
3–30 MHz	100–10 m	HF		
30–300 MHz	10–1 m	VHF		
300–1000 MHz	100–30 cm	UHF		
1–2 GHz	30–15 cm		*L*-band	
2–3 GHz	15–10 cm		*S*-band	
3–4 GHz	10–7.5 cm	SHF		Microwave/lumped passives, transmission lines off-chip
4–8 GHz	7.5–3.75 cm		*C*-band	
8–12.4 GHz	37.5–24 mm		*X*-band	
12.4–18 GHz	24–17 mm		*Ku*-band	
18–26.5 GHz	17–1.1 mm		*K*-band	
26.5–30 GHz	1.1–1 mm		*Ka*-band	
30–40 GHz	<1 mm	EHF		mm-wave/transmission lines on and off chip
40–75 GHz			*V*-band	
75–110 GHz			*W*-band	
110–300 GHz			–	

2.2 Review of Modulation Schemes

As discussed in Chap. 1, the power amplifier is driven by a signal that is generated by a modulation block. Modulation implies that properties of the carrier signal, that is the signal that can physically be amplified and transmitted, are varied so that the information of interest is superimposed [5, 6]. Modulation is accomplished by means of a modulator. On the receiver side, a demodulator is used to recover the same information.

Modern telecommunication systems are moving from employing analog modulation towards employing digital modulation. Thus, various digital modulation schemes are discussed in this review. In a digital modulation scheme, the carrier signal is modulated by a discrete signal. Digital modulation is therefore a type of analog-to-digital conversion. Some basic digital modulation techniques, already defined in Chap. 1, are redefined here for readers' convenience:

- Phase-shift keying (PSK),
- Frequency-shift keying (FSK),
- Phase-amplitude modulation (PAM),

- Quadrature amplitude modulation (QAM),
- On-off keying (OOK),
- Orthogonal frequency-division multiplexing (OFDM), and
- Various direct-sequence spread spectrum (DSSS) techniques.

2.2.1 Phase Shift-Keying

PSK is accomplished by modulating the digital information signal onto the carrier signal by changing its phase. A finite number of phases (M) is used, usually two for bits 0 and 1 (binary PSK or BPSK), four for bit combinations 00, 01, 10 and 11 (QPSK) or eight for eight 3-bit combinations (octal PSK). A typical waveform of BPSK is shown in Fig. 2.1, and signal space diagrams (constellations) of BPSK, QPSK and octal PSK are shown in Fig. 2.2.

2.2.2 Frequency Shift-Keying

FSK is accomplished by modulating the digital information signal onto the carrier signal by changing its frequency. Usually, two discrete frequencies are used to represent zeros and ones of a binary digital signal. This concept is illustrated in Fig. 2.3.

2.2.3 Phase-Amplitude Modulation

In a PAM system, the message is encoded as the amplitude in series of pulses. The number of amplitude levels required is $M = 2^k$ for k-bit blocks of symbols. As in PSK, usually one-bit, two-bit or three-bit symbol combinations are used, corresponding to $M = 2$, 4 and 8 respectively. This concept is illustrated in Fig. 2.4.

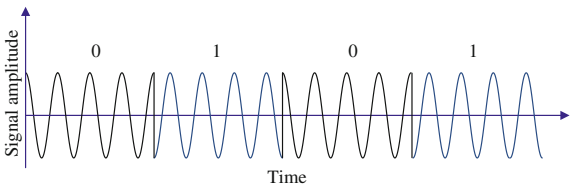

Fig. 2.1 The BPSK waveform

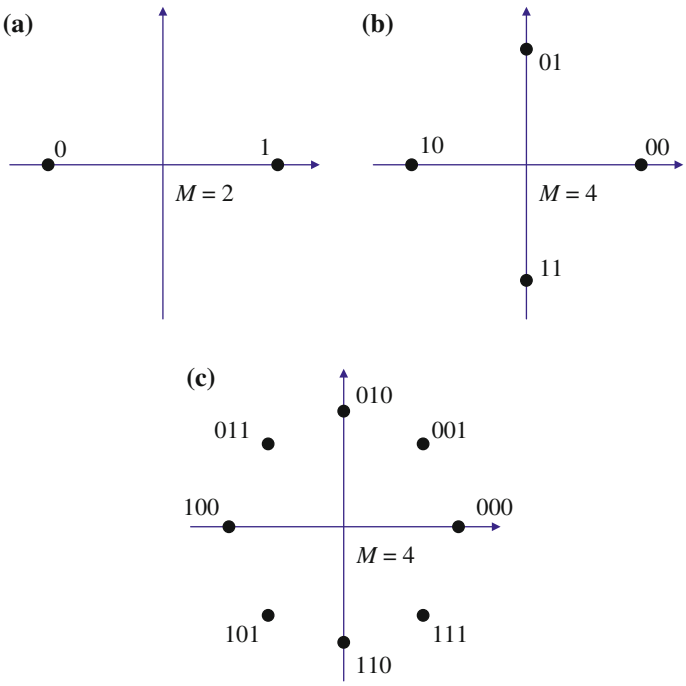

Fig. 2.2 Signal constellations of **a** BPSK, **b** QPSK and **c** octal PSK

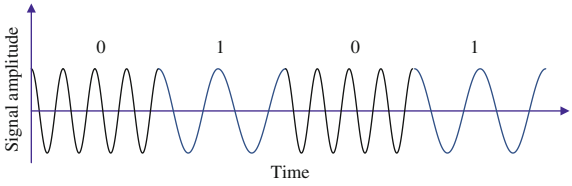

Fig. 2.3 Binary FSK waveform

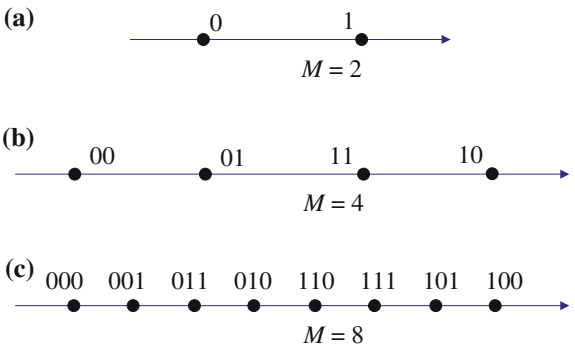

Fig. 2.4 The PAM signal constellations for **a** $M = 2$, **b** $M = 4$ and **c** $M = 8$

2.2.4 Quadrature Amplitude Modulation

QAM is a technique for bandwidth efficiency improvement, where two or more separately modulated signals are combined on the carriers that are out of phase. Thus it is a combination of a PSK scheme with another scheme, usually PAM. When combining M_1-level PAM with M_2-phase PSK, $M = M_1M_2$ combined signal constellation can be created, as illustrated in Fig. 2.5.

2.2.5 On-Off Keying

OOK is the simplest modulation technique. In this scheme, if the carrier signal is present, it indicates a digital one, and if the carrier signal is absent, it indicates a digital zero, as illustrated in Fig. 2.6.

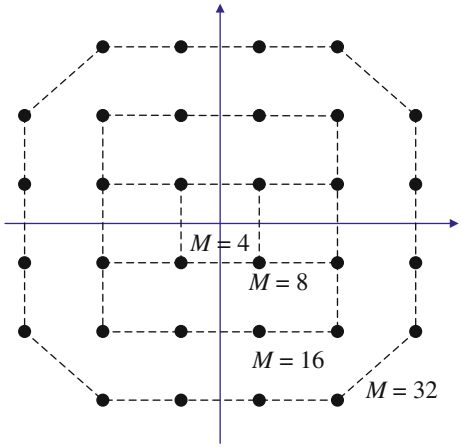

Fig. 2.5 QAM constellations for different values of M

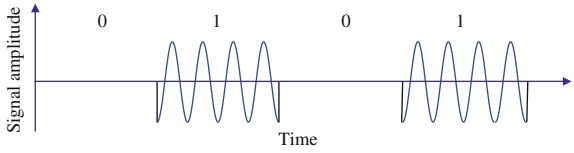

Fig. 2.6 OOK waveform

2.2.6 Orthogonal Frequency-Division Multiplexing

OFDM is a technique used in cases where it is more feasible to transmit data over a large number of carriers simultaneously rather than using a single carrier with a high data rate. This scheme is practical for high data transmission, such as for high-definition television or LTE networks. OFDM combines carriers with the same amplitude and modulation scheme, but separated in frequency so that modulation products arising from one frequency are negligible at the frequencies of the other carriers.

2.3 Antennas and Propagation

After modulation and power amplification, the amplified signal is passed onto an antenna in order to be transmitted. Antennas are therefore an important part of every transmitter and used to radiate the electromagnetic energy into the channel effectively [7]. On the receiving side, antennas are used for receiving the electromagnetic energy from the channel.

Each antenna has characteristic input impedance, which is usually designed to be 50 Ω. For power amplifier design, the antenna efficiency is also important, which is the ratio of radiated power to the power fed to the antenna [2]:

$$\eta_A = \frac{P_{RAD}}{P_{FED}}. \tag{2.2}$$

An antenna also has its radiation characteristics, which are mostly determined by its length and the way in which it is excited. The principle of antenna operation is based on the Ampere-Maxwell's law:

$$\Delta \times \mathbf{H} = \mathbf{J} + \frac{\partial \mathbf{D}}{\partial t}, \tag{2.3}$$

where $\frac{\partial \mathbf{D}}{\partial t}$ is the displacement current, $\mathbf{J}(t)$ is the time varying current density and $\mathbf{H}(t)$ is the time varying magnetic field around the antenna.

The power density at the distance r from the antenna is

$$p(r) = G_T \frac{P_T}{4\pi r^2}, \tag{2.4}$$

where G_T is the gain of the antenna in the particular direction and P_T is the transmitted power. From this equation, it is clear that the power density decreases quadratically with the distance and that high gains are needed to transmit over long distances. The amount of power received by the antenna on the receiver side with gain G_R is given by the Friis formula

$$P_R = \frac{P_T G_T G_R \lambda^2}{(4\pi r)^2}. \tag{2.5}$$

Various types of antennas are commonly used [3]:

- Wire antennas (dipoles, monopoles and others) with low gains, used mostly at HF to UHF,
- Aperture antennas (open-ended waveguides, horns, reflectors) with moderate to high gains, used in microwave or mm-wave bands, and
- Printed antennas on various substrates (slots, dipoles or microstrip) with high gains and also used in microwave or mm-wave bands.

Several antennas can be combined into antenna arrays in order to obtain more directivity and other desirable properties.

The length of an antenna becomes very important when considering packaging, especially when talking about SOP solutions. If an antenna is placed in air, the length of the antenna is proportional to the wavelength. However, if the antenna can be printed in a package, then the length of the antenna scales according to the following equation [8]:

$$l = \frac{\lambda}{\sqrt{\mu_r \varepsilon_r}}, \tag{2.6}$$

where μ_r and ε_r are the relative permeability and permittivity of the substrate on which the antenna is printed. Thus different substrates allow for antennas with different lengths to be placed on SOP which increases the range of options.

For transmission above 30 MHz, propagation is possible only by line-of sight waves. There are two types of these waves: direct waves and ground-reflected waves. Most of the transmissions above HF are accomplished by direct waves. Propagation of waves is influenced by different types of losses, including space loss, atmospheric loss, polarization mismatch loss, impedance mismatch loss and pointing loss.

2.4 The Power Transistor

This section introduces different semiconductor technologies, temperature concerns due to transistor operation and transistor types, and also introduces transistor modeling for power amplification.

2.4.1 Semiconductor Technologies for Transistor Fabrication

Traditionally, several device technologies have been used for fabricating transistors that can be used for power amplification [6, 9, 10]. Initially, gated structures such as MOSFETs, metal-semiconductor field-effect transistors (MESFETs), HEMTs and pseudomorphic HEMTs (pHEMTs) found widespread use. After the introduction of bipolar transistor with a wide-gap emitter, or HBT [11, 12], bipolar transistors emerged as a preferred choice, because of their higher gain and current densities at RF. In the late twentieth century, most of the on-chip power amplifier implementations were deployed with HBTs. Laterally diffused metal oxide semiconductor (LDMOS) transistors are also used for applications below 2 GHz [13]. Figure 2.7 illustrates the relation between different transistors.

In the case of integrated transmitters, this resulted in systems that included at least two ICs in their implementation: a silicon CMOS-based front end and a power amplifier fabricated in another technology. Bipolar complementary metal oxide (BiCMOS) processes are emerging as an alternative to the two-chip integrated solution. This is because it is possible to fabricate both MOSFETs and HBTs in a BiCMOS process, thus allowing BiCMOS technology to bridge the integration gap and reduce the cost of integrated transmitter manufacturing. However, as superior MOSFET technologies emerge, integration in pure CMOS is also becoming practical.

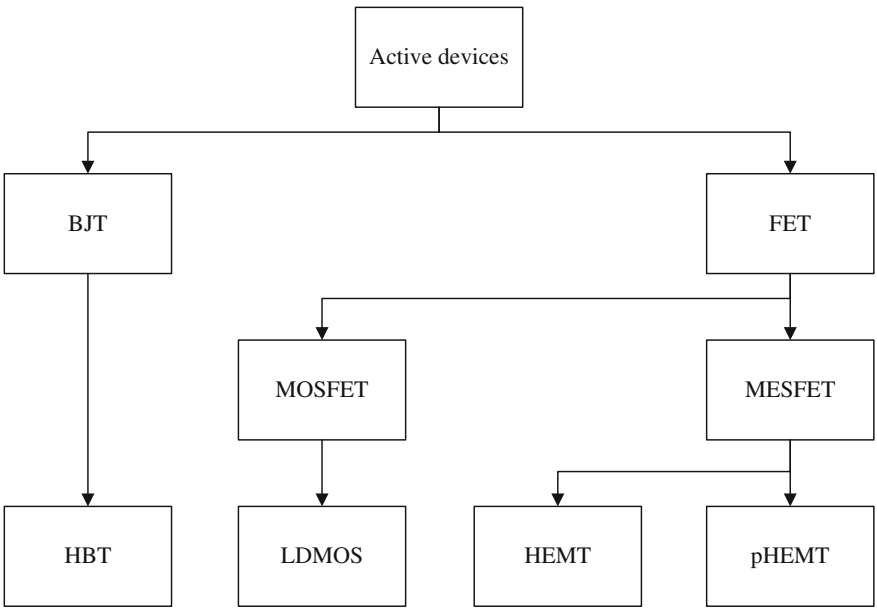

Fig. 2.7 Types of active devices

Table 2.2 Process parameters for Si BJT, SiGe HBT and GaAs HBT technologies [19]

Parameter	Si BJT	SiGe HBT	GaAs HBT
f_T (GHz)	27	44	46
Forward gain, β	100	200	120
Base-emitter voltage, V_{be} (V)	0.8	0.8	1.33
Early voltage, V_A (V)	36	100	1223
Collector-emitter breakdown voltage, V_{ce} (V)	6.2	6	14.3
Collector-base breakdown voltage, V_{cb} (V)	20	12	26
Emitter-base breakdown voltage, V_{eb} (V)	2	5	6.9
Power density (mW/μm$^{2)}$	2	2	0.9
Thermal conductivity (W/cm-°C)	1.5	1.5	0.49
Base-emitter capacitance, C_{be} (fF)	11	10	2.4
Base-collector capacitance, C_{bc} (fF)	3.6	3.3	1
Possibility of NMOS and PMOS integration	Yes	Yes	No

Technologies such as gallium-nitride (GaN), aluminum-gallium-nitride (AlGaN), silicon-carbide (SiC), and indium-phosphate have been struggling for survival in the battle between Si, SiGe and GaAs technologies [9, 14–20]. The AlGaN/GaN is suitable for both high-frequency and high-power designs, but together with the SiC technology it has been sidetracked on the road to microwave applications by technical difficulties and high fabrication costs. The indium-phosphate technology itself does not provide any substantial benefits for the linear power amplifier design.

Table 2.2 shows some typical process parameters for some of the older Si BJT, SiGe and GaAs processes for technology comparison purposes. Silicon technology, as expected, offers the worst process parameters compared to the two HBT technologies. Similar observation is possible by analyzing the PAE, power gain and *S*-parameters obtained from the performance measurement study summarized in Table 2.3.

Emerging technologies can be compared by introducing various figures of merit [2]. Johnson's figure of merit is calculated as

$$JFOM = \frac{E_{BD} v_{sat}}{2\pi}, \tag{2.7}$$

and Baliga's figure of merit is defined as

Table 2.3 Various performance parameters for PAs fabricated in three different technologies (f = 1.88 GHz, V_{CC} = 3.4 V and P_{OUT} = 28 dBm) [19]

Parameter	Si BJT	SiGe HBT	GaAs HBT
PAE (%)	33.1	35	39.3
Gain (dB)	22.1	21.8	27.1
S_{11} (dB)	−13.8	−16.9	−12.6
S_{12} (dB)	20.2	20.5	27.2

Table 2.4 Properties of Si, SiC, GaN and GaAs semiconductors [2]

Property	Unit	Si	SiC	GaN	GaAs
Bandgap energy, E_G	eV	1.12	3.26	3.42	1.42
Electron mobility, μ_n	cm^2/V-s	1360	900	2000	8500
Hole mobility, μ_p	cm^2/V-s	480	120	300	400
Breakdown electric field, E_{BD}	V/cm	2×10^5	2.2×10^6	3.5×10^6	4×10^5
Saturation electron drift velocity, v_{sat}	cm/s	10^7	2.7×10^7	2.5×10^7	1.2×10^7
Relative dielectric constant, ε_r	–	11.7	9.7	9	12.9
Thermal conductivity, k_{th}	W/K-cm	1.5	4.56	1.3	0.55

$$BFOM = \varepsilon_r \varepsilon_0 \mu_n E_G^3, \tag{2.8}$$

where the parameters are defined in Table 2.4 and $\varepsilon_0 = 8.85 \times 10^{-12}$ F/m is the absolute permittivity. Table 2.4 also lists values of these parameters for Si, SiC, GaN and GaAs technologies. These values have been used to form a comparison of JFOM and BFOM of each technology, as shown in Fig. 2.8.

2.4.2 *Temperature Aspects of Transistors*

As mentioned in Chap. 1, excess power dissipated in a transistor due to low efficiency is converted to heat, which decreases the performance of an amplifier [21]. The amount of heat generated and the way in which that heat is dissipated in a power amplifier system depend on the technology in which the IC is fabricated or type of substrate used for discrete implementation, as well as on the type of active device (transistor) used for power amplification.

A MOS transistor is less prone to heating than a BJT (HBT) because of its negative temperature coefficient [6, 21]. This negative coefficient causes the drain current of the MOSFET to decrease with temperature, which allows multiple MOSFETs to be connected in parallel. In HBTs, the situation is reversed. If multiple emitter fingers are used and are not perfectly balanced, the emitter with higher current will tend to take up an even higher proportion of current, which gives rise to local hot spots and possibly permanent device damage. Because current is flowing only in a small hot region, the total gain of the device decreases. Normally, to compensate for this current gain decrease, ballast resistors are added in series with the emitter or base electrodes. This acts as negative feedback, since with the increase in current, the voltage across ballast resistors will also increase,

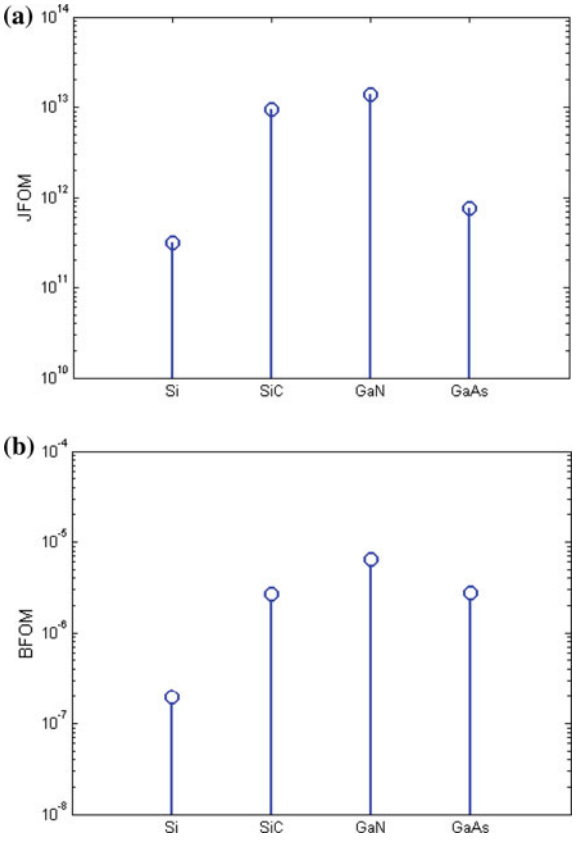

Fig. 2.8 Comparison of **a** JFOM and **b** BFOM of Si, SiC, GaN and GaAs semiconductors [2]

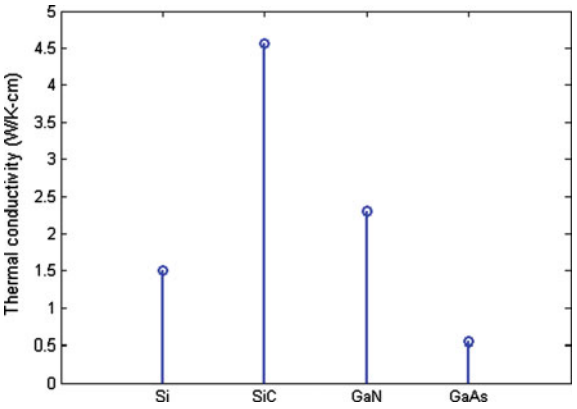

Fig. 2.9 Thermal conductivity of various semiconductor materials

counter-effecting the current increase. Including ballasting resistors, however, decreases the output power, power gain and the efficiency of the amplifier.

Thermal conductivity of various semiconductor materials, listed in Table 2.4, is plotted in Fig. 2.9.

2.4.3 *Transistor Models and Large-Signal Transistor Operation*

Transistor models for a particular technology are usually made available for simulation purposes through a process design kit provided by the foundry. When designing with BJTs, traditionally the Gummel-Poon model was the most popular model for the design of bipolar circuits for a considerable time [22]. Other RF models, such as the Vertical Bipolar Inter-Company (known as VBIC) model for the HBT [23], offer several improvements over the Gummel-Poon model.

For the purpose of this book, however, it is sufficient to use a very simple model of the transistor, with or without specific parasitics as applicable for a particular power amplifier analysis. Throughout this book, in the case of continuous-mode power amplifiers, the transistor is modeled as a dependent current source. In the case of the switch-mode power amplifier, the transistor can be modeled as a simple switch with series resistance (and sufficient gain). When dealing with MOSFETs, the amount of amplification can be set by choosing the transistor width (W) and length (L) parameters. In the case of HBTs, on the other hand, transistor forward gain β is fixed for a chosen transistor, thus an appropriate transistor needs to be selected carefully.

In this section the model and operation of power MOSFET is reviewed, which will be sufficient to analyze any power amplifier stage mentioned later in this book.

2.4.3.1 The Power MOSFET

A high-frequency small signal model of the power MOSFET operating in the pinch-off (saturation) region is shown in Fig. 2.10. For low drain currents, the n-type enhancement-type MOSFET (NMOS) with a long channel and for $v_{GS} \geq V_t$, where v_{GS} is the gate-to-source voltage and V_t is the threshold voltage, is given by a well-known square law:

$$i_D = K(v_{GS} - V_t)^2(1 + \lambda v_{DS}), \tag{2.9}$$

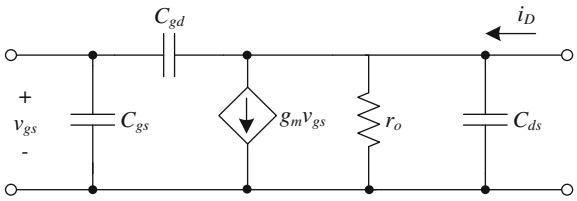

Fig. 2.10 High-frequency model of the high-power MOSFET

where

$$K = \frac{1}{2}\frac{W}{L}\mu_n C_{ox}, \tag{2.10}$$

λ is the channel-length modulation (not to be confused with wavelength) and C_{ox} is the oxide capacitance per unit area of the gate. C_{ox} is defined as

$$C_{ox} = \frac{\varepsilon_{ox}}{t_{ox}}, \tag{2.11}$$

where ε_{ox} is the oxide permittivity and t_{ox} is the oxide thickness.

Channel-length modulation arises because the increase in drain-to-source voltage v_{DS} beyond saturation voltage v_{DSsat} causes the effective channel length to shorten slightly. The relative change is λv_{DS}, as seen in Eq. (2.8). Parameter λ is defined as

$$\lambda = \frac{1}{V_A}, \tag{2.12}$$

where V_A is the MOSFET parameter often referred to as the Early voltage, for the purpose of comparison with BJTs. Channel-length modulation also causes resistance of r_o to appear in the small-signal model shown in Fig. 2.10. If I_D is the DC portion of the drain current, r_o is

$$r_o = \frac{1}{\lambda I_D} = \frac{V_A}{I_D}. \tag{2.13}$$

Transconductance gain g_m, also shown in the small-signal model, is the gain parameter of the transistor applicable to small-signal levels only. It is defined as the derivative of the drain current with respect to gate-to-source voltage, at the point where the transistor is biased (V_{GS}). Thus,

$$g_m = \left.\frac{di_D}{dv_{GS}}\right|_{v_{GS}=V_{GS}} = 2K(V_{GS} - V_t) = 2\sqrt{KI_D}. \tag{2.14}$$

For high drain currents (common in power amplification), NMOS operates according to the linear law, which can be approximated as

$$i_D = K_S(v_{GS} - V_t)(1 + \lambda v_{DS}), \tag{2.15}$$

where

$$K_S = \frac{1}{2}\mu_n C_{ox} W v_{sat}. \tag{2.16}$$

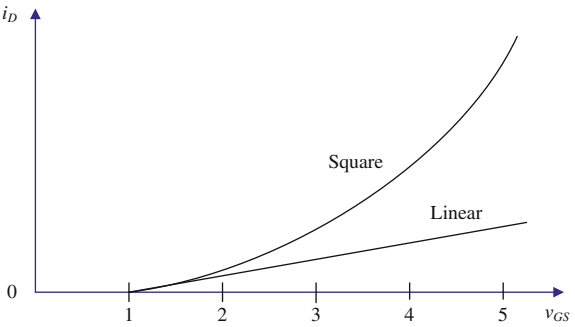

Fig. 2.11 MOSFET linear and square law for V_t = 1 V

The relationship between the square law and the linear is illustrated in Fig. 2.11.

At high frequencies, the effects of the capacitors shown in the model in Fig. 2.10 on the transistor gain become prominent. Current through the gate at high frequencies can be expressed as

$$i_G = j\omega(C_{gs} + C_{gd})v_{GS}, \tag{2.17}$$

where $\omega = 2\pi f$, f is the operating frequency and $j = \sqrt{-1}$. The current gain is then the ratio of the input and output of the current:

$$A(j\omega) = \frac{i_D}{i_G} = \frac{g_m v_{GS}}{j\omega(C_{gs} + C_{gd})v_{GS}} = \frac{g_m}{j\omega(C_{gs} + C_{gd})}. \tag{2.18}$$

An important parameter of any transistor for high frequencies is the unity (0 dB) gain frequency (f_T). It is the frequency at which the magnitude of the short-circuit gain ($|A(j\omega)|$) reaches one (thus making the transistor act as an attenuator instead of an amplifier). For MOSFET, it can be evaluated from

$$\frac{g_m}{2\pi f_T(C_{gs} + C_{gd})} = 1. \tag{2.19}$$

Thus

$$f_T = \frac{g_m}{2\pi(C_{gs} + C_{gd})} = \frac{\sqrt{KI_D}}{\pi(C_{gs} + C_{gd})}. \tag{2.20}$$

The concept of f_T is illustrated in Fig. 2.12.

It is worth noting here that with scaling of technology nodes, transistors with increasing f_T values can be fabricated at the an expense of other parameters, most obviously, the breakdown voltage. This allows for transceiver operation at frequencies much higher than previously possible.

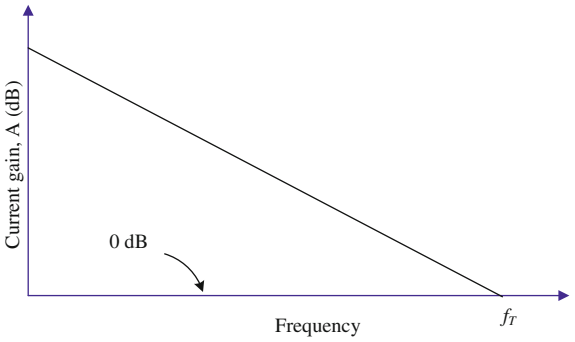

Fig. 2.12 Current gain versus frequency curve of the transistor illustrating the concept of f_T

2.5 Substrates for Discrete Implementations

In integrated designs, substrate refers to a material on which the transistors and other components are deposited, such as Si or SiC, described in the previous section. For discrete power amplifier design, it is important to mention substrates for discrete implementations. When referring to substrates in discrete implementations, one could be referring to [1, 8, 24]:

- Substrates on which discrete components are fabricated (e.g. inductors, capacitors, resistors),
- Substrates for PCBs on which the transmission lines are designed, and
- Substrates for packaged systems and subsystems (SOP).

For discrete components, substrates are chosen so that they exhibit very little parasitic resistance or reactance. Thin-film resistors, for example, are typically produced on alumina or beryllia substrates because they entail a small amount of reactance.

The PCB, which is normally used to support connections of the electronic components mechanically, also features substrates that are non-conductive. Passive components can be laid out on the PCB in the form of microstrip transmission lines. Similar materials are used as the foundation for packaged systems and subsystems. Ceramics and laminates are usually a good option for these PCB-like structures. Different types of ceramic materials, such as high-temperature co-fired alumina or aluminum-nitride with better thermal properties, are available. Hybrid structures, such as laminates that are made of bonded layers, normally with a FR4 material core, may be needed to meet stringent RF requirements.

In SOP, it is also important for the substrate to provide excellent high-frequency electrical properties. It should have good mechanical and chemical resistance and thin-film multilayer capabilities, however, while remaining cost-competitive. Substrate technologies that are able to satisfy these requirements fall under the

Table 2.5 Advantages and disadvantages of using integrated substrates with ICs and discrete substrates with SOP and PCBs in power amplifier design

Type of implementation	Advantages	Disadvantages
IC	• High integration • Small size • Inexpensive	• Low-Q passives • Thermal issues • Lower power
SOP	• Fairly good integration • High density • Moderate- to high-Q passives • High power	• Larger size than that of the IC • Longer time to market than IC • Higher costs
Discrete on PCB	• Readily available • High-Q passives • High power	• Large size • Low density • Component variation

categories of ceramic and organic substrates [8, 24]. Typical ceramic substrates used are low-temperature cofired ceramics and high-temperature cofired ceramics. The organic substrate includes various polymers, including liquid-crystal polymers.

Table 2.5 shows a comparison of advantages and disadvantages between using integrated substrates (ICs), or discrete substrates (on SOP and PCB) in power amplifier design. SOP has more advantages that are not listed in this table, which will be discussed in more detail in Chap. 9 when discussing the packaging of power amplifiers. Kuo et al. also show some performance figures for 5 GHz power amplifiers fabricated on different substrates [25].

2.6 The Smith Chart

The Smith chart is one of the most useful graphical tools available to the RF and microwave designer [1]. It is used to simplify RF and microwave circuit analysis, whereby complex equations can be solved graphically on this chart. An impedance Smith Chart is illustrated in Fig. 2.13. In power amplifier design, the Smith chart can be useful for impedance-to-admittance conversion, as well as for impedance matching, which will be the topic of Chap. 6.

The Smith Chart is basically a combination of a family of constant resistance circles and a family of constant reactance circles, both shown in Fig. 2.14. Each point on the constant resistance or a reactance circle has the same resistance or reactance respectively. A two-port model of a circuit is given in Fig. 1.11 in Chap. 1, where Z_0 is a complex impedance $R = jX$. The reflection coefficient of the load impedance when given a source impedance can be found by formula

$$\rho = \frac{Z_S - Z_L}{Z_S + Z_L} = \frac{Z_0 - 1}{Z_0 + 1}. \tag{2.21}$$

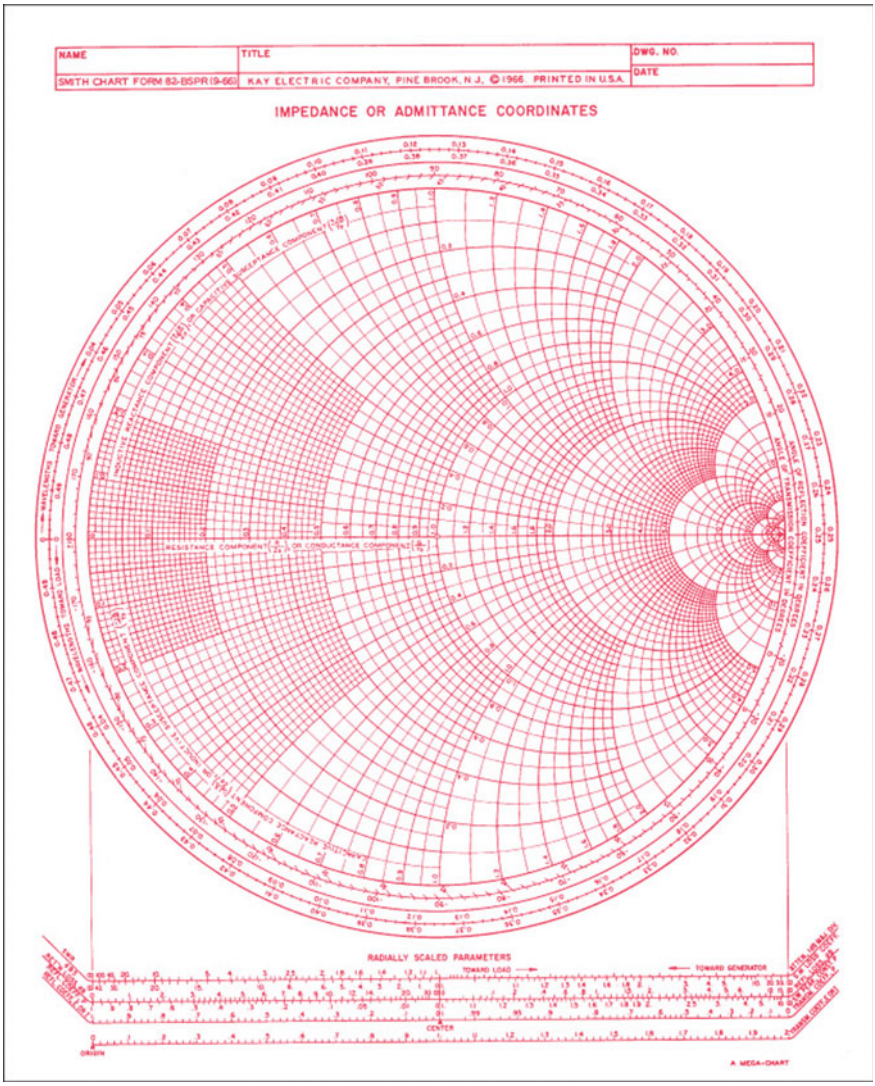

Fig. 2.13 The Smith chart. *Courtesy* Analog Instruments Co.

The polar form of the reflection coefficient is

$$\rho = p + jq = \frac{R + jX - 1}{R + jX + 1}. \tag{2.23}$$

By treating real and imaginary parts separately and removing X from the above equation, the equation for the constant resistance circle is obtained:

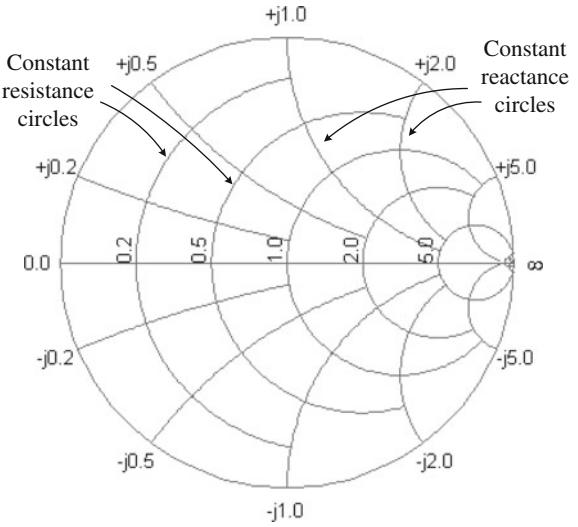

Fig. 2.14 Constant resistance and reactance circles

$$\left(p - \frac{R}{R+1}\right)^2 + q^2 = \left(\frac{1}{R+1}\right)^2, \tag{2.23}$$

with the circuit centers at $p = R/(R + 1)$ and $q = 0$, and radii equal to $1/(R + 1)$. Similarly, by removing R from the same equation, the constant reactance circle is obtained:

$$(p-1)^2 + \left(q - \frac{1}{X}\right)^2 = \left(\frac{1}{X}\right)^2, \tag{2.24}$$

with the circuit centers at $p = 1$, $q = 1/X$ and radii of $1/X$.

All the circuits have one common intersecting point at coordinate (1, 0). The largest circle is the zero resistance circle and the outer boundary of the Smith chart, and the infinite resistance circle is reduced to a point at (1, 0). To plot the impedances on the Smith chart, the impedances must first be normalized by a certain value. For example, this value could be the characteristic impedance of the transmission line. The concept of characteristic impedance is defined in Chap. 5, and it could be 50 Ω. Thus, if impedance $(50 + j25)$ Ω is to be manipulated on the Smith chart, one would typically plot a value of $(1 + j0.5)$ Ω. An example of impedance manipulation on the Smith chart will be presented in the next section when showing how to convert impedance into admittance. Several more examples will be presented in Chap. 6 when dealing with impedance matching.

Recently, a 3-D version of the Smith chart was reported [26]. It is based on the extended complex plane (Riemann sphere). The north pole is the perfect matching point, while the south pole is the perfect mismatch point.

2.7 Admittance (Y-) and Scattering (S-) Parameters

2.7.1 Y-Parameters

Admittance is defined as the reciprocal of the impedance [1]:

$$Y = \frac{1}{Z} = G \pm jB, \tag{2.25}$$

where G is the conductance and B is the susceptance, both expressed in siemens (S). On the Smith chart, any impedance can be converted to admittance by plotting the impedance on the chart and drawing a straight line from the plotted point through the origin of the graph. The admittance is then at the point on the same line, and the same distance from the origin but on the other side. This essentially means that the Smith chart can simply be flipped over. Let us illustrate this by means of an example, where we want to convert an impedance of $(50 + j25)\ \Omega$ into admittance. First we start by normalizing the value by a factor of 50, thus we need to plot $(1 + j0.5)\ \Omega$. Then we draw a line through the center of the graph, and extend it to the other side of the graph. The value that is read off at that point is $(0.8 - j0.4)$ S. If we normalize it back with the factor of 50 we obtain $(0.016 - j0.008)$ S (note that for the admittance we have to divide by 50). This process is illustrated in Fig. 2.15. To verify the procedure, we can use Eq. (2.25):

$$\begin{aligned} Y = \frac{1}{Z} = \frac{1}{50 + j25} = \frac{50 - j25}{(50 + j25)(50 - j25)} = \frac{50 - j25}{50^2 + 25^2} = \frac{50 - j25}{3125} \\ = (0.016 - j0.008)\ \text{S}. \end{aligned}$$

As mentioned, the Smith chart shown in Fig. 2.13 is the impedance Smith chart, but from previous calculations it became evident that if we rotate the chart by 180º, the chart becomes an impedance chart. If we now overlay the impedance and admittance Smith charts, we get the impedance-admittance Smith chart, which is extremely useful for impedance matching, as will be seen later in Chap. 6.

The admittance parameters (Y-parameters) of a two-port network were introduced as a tool to present the characteristics of an amplifier unambiguously at a certain frequency. An amplifier as a two-port black box with Y-parameters is shown

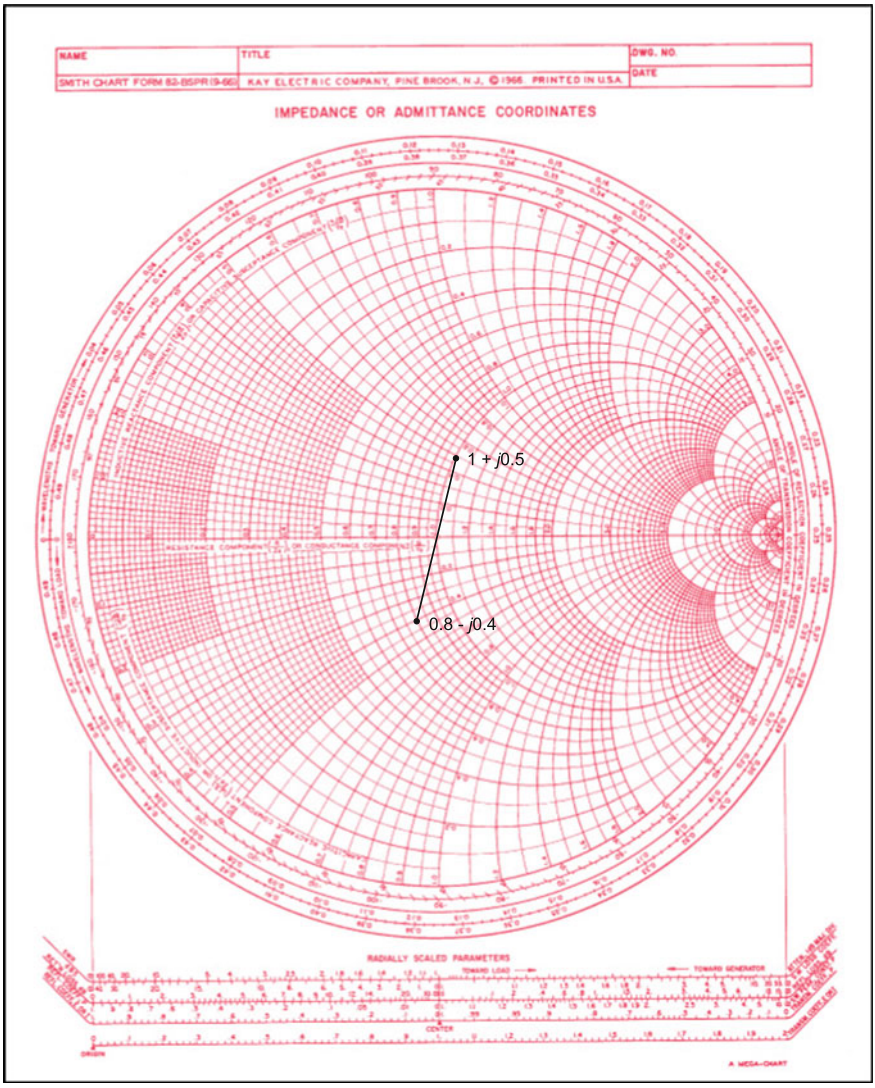

Fig. 2.15 Illustration of impedance to admittance conversion using the Smith chart

in Fig. 2.16, where I_1 and V_1 are the input current and voltage and I_2 and V_2 are the output current and voltage. The short-circuit Y-parameters are then by definition:

$$y_i = \left.\frac{I_1}{V_1}\right|_{V_2=0}, \tag{2.26}$$

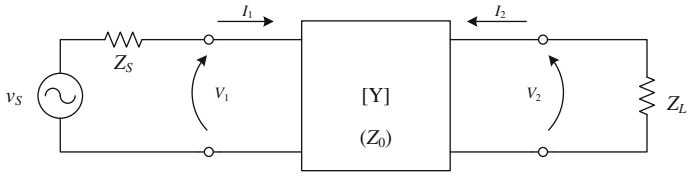

Fig. 2.16 Two port Y-parameter network

$$y_r = \left.\frac{I_1}{V_2}\right|_{V_1=0}, \tag{2.27}$$

$$y_f = \left.\frac{I_2}{V_1}\right|_{V_2=0}, \tag{2.28}$$

and

$$y_o = \left.\frac{I_2}{V_2}\right|_{V_1=0}, \tag{2.29}$$

where y_i is the short-circuit input admittance, y_r is the short-circuit reverse transfer admittance, y_f is the short-circuit forward transfer admittance and y_o is the short-circuit output admittance. Thus,

$$I_1 = y_i V_1 + y_r V_2, \tag{2.30}$$

and

$$I_2 = y_f V_1 + y_o V_2. \tag{2.31}$$

2.7.2 S-Parameters

Scattering parameters (*S*-parameters) are much easier to measure and work with than *Y*-parameters. *S*-parameters are also more intuitive than *Y*-parameters, since they are the measure of the reflection and gain, as opposed to being a measure of a just an abstract quantity such as admittance. Scattering parameters can be defined with the aid of Fig. 2.17, which is identical to Fig. 1.11, but with incident and reflected waves shown instead of source and load reflection coefficients.

A travelling wave has the following characteristics [1]:

1. A part of the traveling wave originating from the source and incident upon the two-port device (a_1) will be reflected as b_1 and another part will be transmitted through the two-port device;

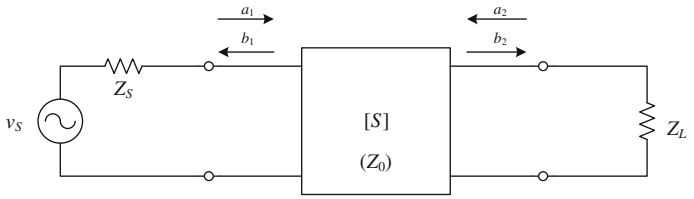

Fig. 2.17 *S*-parameter two-port model with incident and reflected waves shown

2. A part of the transmitted signal is reflected from the load and becomes incident upon the output of the two-port device (a_2); and
3. A part of the signal (a_2) is reflected from the output port back toward the load as b_2 and another part is transmitted through the two-port device back to the source.

This indicates a need for two reflection coefficients (S_{11} and S_{22}) and two gain coefficients. Thus, the input port reflection coefficient S_{11} is defined as

$$S_{11} = \left.\frac{b_1}{a_1}\right|_{a_2=0}, \tag{2.32}$$

the output port reflection coefficient S_{22} is

$$S_{22} = \left.\frac{b_2}{a_2}\right|_{a_1=0}, \tag{2.33}$$

the forward gain coefficient is

$$S_{21} = \left.\frac{b_2}{a_1}\right|_{a_2=0}, \tag{2.34}$$

and the reverse gain coefficient is

$$S_{12} = \left.\frac{b_1}{a_2}\right|_{a_1=0}. \tag{2.35}$$

Finally, the following two equations can be set

$$b_1 = S_{11}a_1 + S_{12}a_2, \tag{2.36}$$

and

$$b_2 = S_{21}a_1 + S_{22}a_2. \tag{2.37}$$

2.7.3 Conversion Between Y-Parameters and S-Parameters

Conversion between *Y*-parameters and *S*-parameters is fairly simple when conversion formulas are known. To obtain *S*-parameters from *Y*-parameters, the following equations are used:

$$S_{11} = \frac{(1-y_i)(1+y_o)+y_r y_f}{(1+y_i)(1+y_o)-y_r y_f}, \tag{2.38}$$

$$S_{12} = \frac{-2y_r}{(1+y_i)(1+y_o)-y_r y_f}, \tag{2.39}$$

$$S_{21} = \frac{-2y_f}{(1+y_i)(1+y_o)-y_r y_f}, \tag{2.40}$$

and

$$S_{22} = \frac{(1+y_i)(1-y_o)+y_r y_f}{(1+y_i)(1+y_o)-y_r y_f}. \tag{2.41}$$

To obtain *Y*-parameters from *S*-parameters, the following equations are used:

$$y_i = \frac{(1+S_{22})(1-S_{11})+S_{12}S_{21}}{(1+S_{11})(1+S_{22})-S_{12}S_{21}} \cdot \frac{1}{Z_0}, \tag{2.42}$$

$$y_r = \frac{-2S_{12}}{(1+S_{11})(1+S_{22})-S_{12}S_{21}} \cdot \frac{1}{Z_0}, \tag{2.43}$$

$$y_f = \frac{-2S_{21}}{(1+S_{11})(1+S_{22})-S_{12}S_{21}} \cdot \frac{1}{Z_0}, \tag{2.44}$$

and

$$y_o = \frac{(1+S_{11})(1-S_{22})+S_{12}S_{21}}{(1+S_{11})(1+S_{22})-S_{12}S_{21}} \cdot \frac{1}{Z_0}. \tag{2.45}$$

2.8 Resonant Circuits

The resonant circuit is commonly used in power amplifiers to selectively pass a frequency or a group of frequencies while attenuating all other frequencies [1, 2, 27]. It is essentially a band-pass filter (BPF) and is characterized by bandwidth. A typical BPF response is shown in Fig. 2.18. The resonant circuit can be

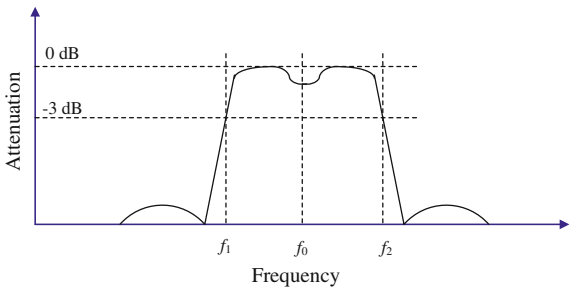

Fig. 2.18 A typical BPF response

implemented by either lumped elements or transmission lines. In this book we stick to lumped elements and parallel and series resonant circuits.

2.8.1 Bandwidth

The bandwidth of the resonant circuit is the difference between the upper frequency f_2 and lower frequency f_1, which mark the point where the magnitude of signal passing through the resonator is 3 dB below (a half of) the maximum signal magnitude:

$$BW = f_2 - f_1. \tag{2.46}$$

2.8.2 Resonant Frequency

A circuit diagram of a parallel resonant circuit is shown in Fig. 2.19.

The reactance of capacitor C at any frequency is

$$X_C = \frac{1}{\omega C}, \tag{2.47}$$

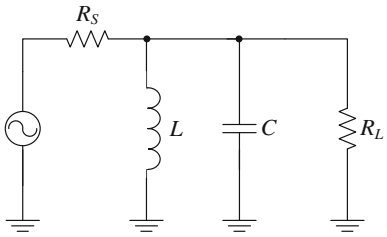

Fig. 2.19 Schematic of a parallel resonant circuit

where $\omega = 2\pi f$ is the angular frequency. The reactance of the inductor is

$$X_L = \omega L. \tag{2.48}$$

Resonance is achieved at the frequency where both reactances are equal:

$$X_C = X_L = \frac{1}{\omega C} = \omega L. \tag{2.49}$$

Resonant frequency is then

$$f_o = \frac{1}{2\pi\sqrt{LC}}. \tag{2.50}$$

Assuming that the combined reactance of the capacitor and inductor close to resonance is sufficiently small so that load resistance in parallel can be ignored, the magnitude of the output voltage of the resonant circuit, V_{out}, in terms of the magnitude input voltage V_{in} is

$$V_{out} = \frac{Z_C || Z_L}{R_S + Z_C || Z_L} V_{in}, \tag{2.51}$$

where $Z = jX$ is the impedance of a capacitor or inductor. Thus, the attenuation at any frequency ω is

$$\frac{V_{out}}{V_{in}} = \left| \frac{j\omega L}{R_S - \omega^2 R_S LC + j\omega L} \right|. \tag{2.52}$$

At ω_o,

$$\frac{V_{out}}{V_{in}} = 1 \tag{2.53}$$

which was expected from the definition of the resonant circuit.

In practice, the load and/or source resistances are not much larger than the reactances of the capacitor and inductor, thus increasing the difficulty of the resonant circuit design. One solution is to use impedance transformation in order to increase the apparent value of resistance. Various power amplifier stages use this method by design.

2.8.3 Quality Factor

The quality factor or Q-factor of the resonant circuit is the ratio of the center frequency of the resonant circuit to its 3-dB bandwidth:

$$Q = \frac{f_o}{BW}. \tag{2.54}$$

The quality factor of the circuit is often called a loaded Q-factor (Q_L) because it describes the passband characteristics of the resonant circuit under loaded conditions. The loaded Q-factor is influenced by both the resistance of the previous circuit stage (source) and the resistance of the following circuit stage (load), and either the inductive or capacitive reactance:

$$Q = \frac{R_p}{X_p}. \tag{2.55}$$

In the case of a power amplifier, the resonant circuit is usually followed by the antenna with resistance of R = 50 Ω, and preceded by a driving transistor with output resistance r_o, which is much larger, thus

$$R_p = R||r_o \approx R. \tag{2.56}$$

2.8.4 Component Quality Factor

The loaded Q-factor should not be confused with the Q-factor of an inductor or a capacitor, which will be discussed later in Chap. 5. However, the Q-factor of each passive influences the loaded quality factor. If a lossy passive with serial reactance X_s and serial resistance R_s is used in a resonant circuit, the additional parallel resistance seen by the circuit will be

$$R_p = (Q_{comp}^2 + 1)R_s \tag{2.57}$$

and the equivalent reactance of that component will be

$$X_p = \frac{R_p}{Q_{comp}}. \tag{2.58}$$

For $Q_{comp} >> 1$, $X_p \approx X_s$. Thus, in order for the resistance of components to be as large as possible and reactance to remain unchanged from specified values, components should have high Q values.

2.8.5 Insertion Loss

Insertion loss is the amount of attenuation due to a component or a group of components inserted between a source and a load. In the resonant circuit, it arises

from resistive losses of the inductor and capacitor. It is closely related to the component Q-factor, discussed earlier.

2.8.6 Coupling of Resonant Circuits

If a single resonant circuit is not sufficient for a particular application, resonant circuits can be coupled together to achieve steeper passband skirts. The choice among capacitive coupling (Fig. 2.20a), inductive coupling (Fig. 2.20b), transformer coupling (Fig. 2.20c) or active coupling (Fig. 2.20d) will depend on the type of application.

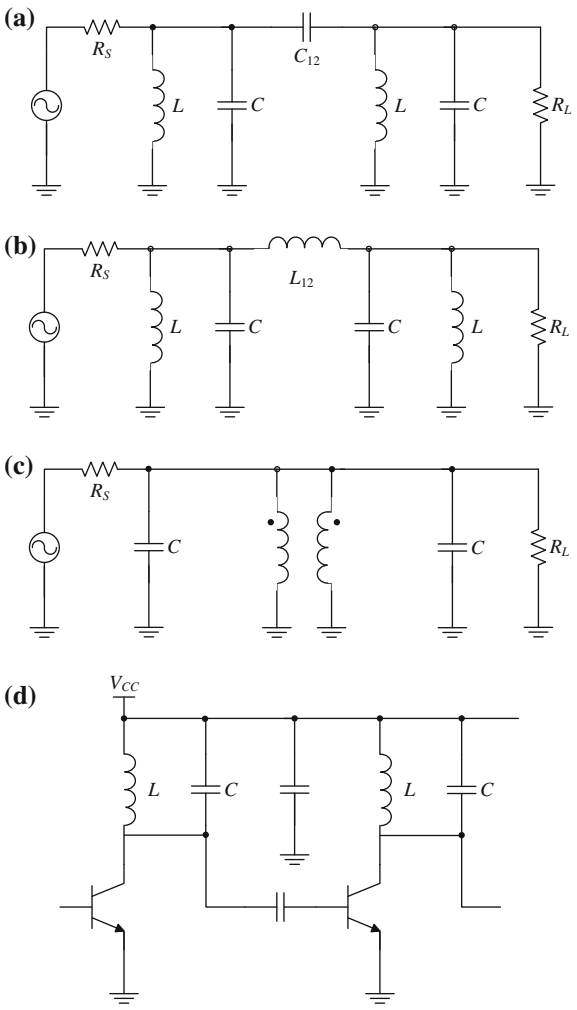

Fig. 2.20 Different ways of resonant circuit coupling: **a** capacitive coupling, **b** inductor coupling, **c** transformer coupling and **d** transistor coupling

For capacitive coupling, the value of capacitance to couple two identical resonant circuits is

$$C_{12} = \frac{C}{Q_L}, \tag{2.59}$$

where C is the resonant circuit capacitance and Q_L is the loaded Q factor of a single resonator. Similarly, for inductive coupling, the combined inductance is

$$L_{12} = Q_L L, \tag{2.60}$$

where L is the resonant circuit inductance.

Active coupling is accomplished by using a transistor. The combined Q is

$$Q_{total} = \frac{Q_L}{\left(2^{1/n} - 1\right)^{1/2}}, \tag{2.61}$$

where n is the number of resonant circuits.

2.9 Fourier Analysis of Periodic Signals

Periodic signals are used to analyze power amplifier output stages. A function is periodic if the following is satisfied [2]:

$$f(\omega t) = f(\omega t \pm 2\pi n). \tag{2.62}$$

Any periodic function can be expressed as an infinite sum of sinusoidal signals, called Fourier series. Fourier analysis is thus used to calculate the DC and harmonic components of periodic signals throughout this book and is discussed here.

Function $f(\omega t)$ can be expressed as

$$\begin{aligned} f(\omega t) = a_0 + \sum_{n=1}^{\infty} (a_n \cos n\omega t + b_n \sin n\omega t) = a_0 + a_1 \cos \omega t + b_1 \sin \omega t \\ + a_2 \cos 2\omega t + b_2 \sin 2\omega t + a_3 \cos 3\omega t + b_3 \sin 3\omega t \\ + a_n \cos n\omega t + b_n \sin n\omega t, \end{aligned} \tag{2.63}$$

where a_n and b_n are called Fourier coefficients and can be calculated for one cycle from

$$a_0 = \frac{1}{T}\int_0^T f(t)dt = \frac{1}{2\pi}\int_0^{2\pi} f(\omega t)d(\omega t), \tag{2.64}$$

$$a_n = \frac{2}{T}\int_0^T f(t)\cos ntd(t) = \frac{1}{\pi}\int_0^{2\pi} f(\omega t)\cos n\omega td(\omega t) \tag{2.65}$$

and

$$b_n = \frac{2}{T}\int_0^T f(t)\sin ntdt = \frac{1}{\pi}\int_0^{2\pi} f(\omega t)\sin\, n\omega\, td(\omega t). \tag{2.66}$$

Two special cases of function in Eq. (2.63) will be used often. If the function $f(\omega t)$ is odd, meaning that $f(\omega t) = -f(\omega t)$, then the calculation of coefficients simplifies to

$$a_0 = a_n = 0, \tag{2.67}$$

and

$$b_n = \frac{4}{T}\int_0^{T/2} f(t)\sin\, n\omega tdt = \frac{2}{\pi}\int_0^{\pi} f(\omega t)\sin\, n\omega td(\omega t). \tag{2.68}$$

Sine function is an example of an odd function. If the same function is even, meaning that $f(\omega t) = f(-\omega t)$, then

$$a_0 = \frac{2}{T}\int_0^T f(t)dt = \frac{1}{\pi}\int_0^{2\pi} f(\omega t)d(\omega t), \tag{2.69}$$

$$a_n = \frac{4}{T}\int_0^{T/2} f(t)\cos ntdt = \frac{2}{\pi}\int_0^{\pi} f(\omega t)\cos n\omega td(\omega t) \tag{2.70}$$

and

$$b_n = 0. \tag{2.71}$$

An example of an even function is the cosine function. Since both sine and cosine functions are defined with an arbitrary origin, it can be shifted on the time axis to simplify the analysis where necessary.

2.10 Summary

In this chapter we reviewed the frequency spectrum and identified that the frequency bands mentioned in the title of the book occupy frequencies between 2 and 18 GHz, where typically the power amplifiers can be implemented with lumped passives, and that transmission lines, if needed, can be implemented in discrete implementations. We reviewed the modulation schemes, where we presented constellations and/or waveforms for PSK, FSK, QAM, OOK and OFDM schemes. Power amplifiers are typically used to drive antennas, thus we discussed some basic antenna concepts. Technologies and substrates for systems-on-chip, SOP and discrete implementations were also discussed, where we concluded that each implementation has its advantages and disadvantages. Some practical aspects of various implementations and packaging will form part of more discussions in Chap. 9. We also presented the theory behind the active device, but we leave the discussion of passives until Chap. 5. The Smith chart was presented as an excellent graphical tool for various RF and microwave calculations, and we demonstrated its power in impedance-to-admittance conversions. However, we will use the Smith chart again in Chap. 6 with impedance matching. Defining equations of *S*- and *Y*-parameters were also given here. Various aspects of resonant circuits were discussed, as these form the basic building blocks of any power amplifier. Fourier analysis, necessary for the analysis of the power amplifier waveforms, was also discussed.

Theory presented in this chapter laid the groundwork for Chaps. 3 and 4, where various aspects will be used when defining and describing different power amplifier output stages. Although some of the concepts presented in this chapter are not paramount to understanding Part 2 of this book, they add to the better understanding of power amplifier application.

References

1. Bowick C, Blyler J, Ajluni C. RF circuit design. 2nd ed. Burlington: Elsevier; 2008.
2. Kazimierczuk MK. RF power amplifiers. 2nd ed. Chiechester: Wiley; 2015.
3. Pozar M. Microwave engineering. 4th ed. Hoboken: Wiley; 2012.
4. International Telecommunication Union. Nomenclature of the frequency and wavelength bands used in telecommunications. ITU-R Recommendation V.431 [Internet]. 2000 May [cited 2015 May 19]. Available from: http://www.itu.int/rec/R-REC-V.431/en.
5. Proakis JG, Salehi M. Digital communications. 5th ed. New York: McGraw-Hill; 2008.
6. Raab FH, Asbeck P, Kenington PB, Cripps S, Popovic ZB, Pothecary N, Sevic JF, Sokal NO. RF and microwave power amplifier and transmitter technologies—part 1. High Freq Electron. 2003;2:22–36.
7. Cheng DK. Fundamentals of engineering electromagnetics. 1st ed. Reading: Addison-Wesley Publishing Company; 1993.
8. Tummala RR, Swaminathan M. System-on-package: miniaturization of the entire system. 1st ed. New York: McGraw-Hill Professional; 2008.
9. Poulin D. The III-V vs. silicon battle. Microw J. 2009;52(4):22–38.

10. Johnson JB, Joseph AJ, Sheridan DC, Maladi RM, Brandt PO, Persson J, Andersson J, Bjomeklett A, Persson U, Abasi F, et al. Silicon-Germanium BiCMOS HBT technology for wireless power amplifier applications. IEEE J Solid-State Circuits. 2004;39(10):1605–14.
11. Kroemer H. Heterostructure bipolar transistors and integrated circuits. Proc IEEE. 1982;70 (1):13–25.
12. Chiou HK, Liao HY, Chen CC, Wang SM, Chen CC. A, 2.6-GHz fully integrated CMOS power amplifier using power combining transformer. Microw Opt Technol Lett. 2010;52 (2):299–302.
13. Cripps SC. RF power amplifiers for wireless communications. Norwood: Artech House; 2006.
14. Avenier G, Diop M, Chevalier P, Troillard G, Loubet N, Bouvier J, Depoyan L. 0.13 m SiGe BiCMOS technology fully dedicated to mm-wave applications. IEEE J Solid-State Circuits. 2009;44(9):2312–21.
15. Nikandish G, Medi A. A design procedure for high-efficiency and compact-size 5–10-W MMIC power amplifiers in GaAs pHEMT technology. IEEE Trans Microw Theory Tech. 2013;61(8):2922–33.
16. Sheppard ST, Doverspike K, Pribble WL, Allen ST, Palmour JW, Kehias LT, Jenkins TJ. High-power microwave GaN/AlGaN HEMTs on semi-insulating silicon carbide substrates. IEEE Electron Device Lett. 1999;20(4):161–3.
17. Nguyen C, Micovic M. The state-of-the-art of GaAs and InP power devices and amplifiers. IEEE Trans Electron Devices. 2001;48(3):472–8.
18. Pribble WL, Palmour W, Sheppard ST, Smith RP, Allen ST, Smith TJ, Ring Z, Sumakeris JJ, Saxler AW, Milligan JW. Applications of SiC MESFETs and GaN HEMTs in power amplifier design. In: 2002 IEEE MTT-S International Microwave Symposium Digest; 2002; Seattle. p. 1819–22.
19. Nellis K, Zampardi P. A comparison of linear handset power amplifier in different bipolar technologies. IEEE J Solid-State Circuits. 2004;39(10):1746–54.
20. Vitusevich SA, Kurakin AM, Klein N, Petrychuk MV, Naumov AV, Belyaev AE. AlGaN/GaN high electron mobility transistor structures: self-heating effect and performance degradation. IEEE Trans Device Mater Reliab. 2008;8(3):543–8.
21. Dongyue J, Wanrong Z, Pei S, Hongyun X, Yang W, Wei Z, Lijian H, Yongping S, Jia L, Junning G. Multi-finger power SiGe HBTs for thermal stability enhancement over a wide biasing range. Solid-State Electron. 2008;52(6):937–40.
22. Degachi L, Ghannouchi F. An augmented small-signal HBT model with its analytical based parameter extraction technique. IEEE Trans Electron Devices. 2008;55(4):968–72.
23. Corporation IBM. BiCMOS7WL design manual. Armonk: IBM Corporation; 2008.
24. Greig WJ. Integrated circuit packaging, assembly and interconnections. 1st ed. New York: Springer; 2007.
25. Kuo CC, Hsu YW, Huang WC, Wang H, Lu H. Performance comparison of flip-chip-assembled 5-GHz 0.18-CMOS power amplifiers on different packaging substrates. IEEE. Trans Compon Packag Manuf Technol. 2013;3(12):2014–21.
26. Muller AA, Soto P, Dascalu D, Neculoiu D, Boria VE. A 3-D smith chart based on the riemann sphere for active and passive microwave circuits. IEEE Microw Wirel Compon Lett. 2011;21(6):286–8.
27. Grebennikov A, Sokal NO, Franco MJ. Switchmode RF and microwave power amplifiers. 2nd ed. Burlington: Elsevier; 2012.

http://www.springer.com/978-3-319-28375-3

Power Amplifiers for the S-, C-, X- and Ku-bands
An EDA Perspective
Božanić, M.; Sinha, S.
2016, XIX, 337 p. 305 illus. in color., Hardcover
ISBN: 978-3-319-28375-3